Published in Applied Physics Letters 78, 1964-1966, 2001
which should be used for any reference to this work


# Continuous wave operation of a 9.3 $\mu$m quantum cascade laser on a Peltier cooler

Daniel Hofstetter,[a] Mattias Beck, Thierry Aellen, and Jérôme Faist
*University of Neuchâtel, Institute of Physics, 1 Rue A.-L. Breguet, Neuchâtel, CH 2000, Switzerland*
Ursula Oesterle and Marc Ilegems
*IMO, Physics Department, EPFL, Ecublens, 1015 Lausanne, Switzerland*
Emilio Gini and Hans Melchior
*Institute of Quantum Electronics, ETHZ, 8093 Zürich, Switzerland*

High average power quantum cascade lasers at 9.3 $\mu$m using InP top cladding layers and both junction up and junction down mounting are presented. A 3 mm long, junction up mounted device emitted 54 mW average power at 30 °C and 11.5% duty cycle with a threshold current density of 3.72 kA/cm$^2$. A similar, but only 1.5 mm long device with high reflection coating on both facets was mounted junction down and tested at even higher duty cycles. At −27 °C, we achieved continuous wave operation with a threshold current density of 3.3 kA/cm$^2$

Midinfrared quantum cascade (QC) lasers have reached a high level of maturity and are now commercially available. They are the ideal light source for environmental and medical sensors.[1–4] Many of those applications call upon high average output powers; this is particularly true for photoacoustic trace gas spectroscopy in the parts per billion concentration range. Up to this point, the highest average output powers were achieved by using superlattice active region QC lasers with an InP lower cladding and an InAlAs-based top cladding layer.[5,6] Additional performance improvements are expected by lowering the thermal resistance of the devices. This can be accomplished by the use of an InP top cladding, by epitaxial side down mounting and the use of buried heterostructure (BH) lasers.[7–10] In this letter, we present our latest results on vertical transition QC lasers at 9.3 $\mu$m which were fabricated with InP top cladding layers. In addition, we improved the thermal resistance of the devices by junction down mounting.

Up to the active region, growth of this material was based on molecular beam epitaxy (MBE) of lattice matched InGaAs/InAlAs layers on top of an *n*-doped InP (Si, $2\times10^{17}\,\mathrm{cm}^{-3}$) substrate. After the waveguide core with the active region, an epitaxial overgrowth by metalorganic vapor phase epitaxy (MOVPE) of the InP top cladding and contact layers completed the growth. The MBE growth process started with the lower waveguide layer (InGaAs, Si, $6\times10^{16}\,\mathrm{cm}^{-3}$, total thickness 0.225 $\mu$m), proceeded with an active region (thickness 1.82 $\mu$m) and was finished by an upper waveguide layer (InGaAs, Si, $6\times10^{16}\,\mathrm{cm}^{-3}$, thickness 0.23 $\mu$m). After thorough cleaning of the surface in $H_2SO_4$, the samples were transferred to an MOVPE system, where the top cladding layer (InP, Si, $1\times10^{17}\,\mathrm{cm}^{-3}$, thickness 2.5 $\mu$m), the contact layer (InP, Si, $7\times10^{18}\,\mathrm{cm}^{-3}$, thickness 0.85 $\mu$m), and the cap layer (InP, Si, $1\times10^{20}\,\mathrm{cm}^{-3}$, thickness 10 nm) were grown. The active region, which formed the central part of the waveguide, consisted of 35 periods; those were alternating *n*-doped funnel injector regions and undoped four quantum well (QW) active regions. The laser transition in the latter was vertical and the lower lasing level utilized a double phonon resonance like the device outlined in reference.[11] Like in a superlattice active region, this four QW design makes use of the short lifetime of the lower laser level. On the other hand, the thin QW right behind the injection barrier guarantees a good injection efficiency, similar as in the diagonal, anticrossed three QW active region.[12] The layer sequence of the structure, in nanometers, and starting from the injection barrier, is as follows: 3.4/**1.4**/3.3/**1.3**/3.2/**1.5**/3.1/**1.9**/3.0/**2.3**/2.9/**2.5**/2.9/**4.0**/1.9/**0.7**/5.8/**0.9**/5.7/**0.9**/5.0/**2.2** nm. $In_{0.52}Al_{0.48}As$ barrier layers are in bold, $In_{0.53}Ga_{0.47}As$ well layers are in roman, and *n*-doped layers (Si $4\times10^{17}\,\mathrm{cm}^{-3}$ for S1840 and Si $2.5\times10^{17}\,\mathrm{cm}^{-3}$ for S1850) are underlined. Laser fabrication proceeded then by standard processing steps like outlined in Ref. 2. Device S1840 was mounted junction up on a copper heatsink, while S1850 was soldered junction down to improve thermal resistance. In both cases, a 2 $\mu$m thick thermally evaporated In layer was used for soldering.

For testing, the devices were placed into a Peltier-cooled aluminum box with a antireflection coated ZnSe window (Alpes Lasers SA). Average output power and voltage vs current ($L-I-V$) curves at temperatures of −30, 0, 30, and 60 °C were measured in this configuration. A pulse length of 40 ns was used with a variable pulse repetition frequency in order to achieve a duty cycle between 1.5%($f_{\mathrm{rep}}=375\,\mathrm{kHz}$) and 20%($f_{\mathrm{rep}}=5\,\mathrm{MHz}$). For higher duty cycles, we left the repetition frequency constant at 5 MHz and changed the pulse length from 40 up to 200 ns. The average output power was measured using a calibrated thermopile detector. For the acquisition of emission spectra, we collected the light with a Au-coated parabolic off-axis mirror (60°, $f$/1.33). After reflection on a second parabolic mirror (90°, $f$/3.75), the light

[a]Electronic mail: daniel.hofstetter@unine.ch

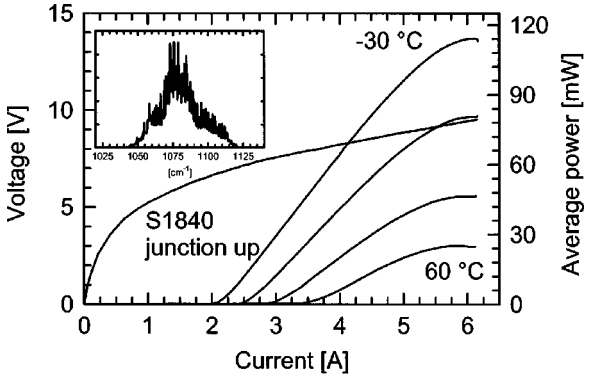


FIG. 1. Light vs current and voltage vs current curves of a 3 mm long and 28 $\mu$m wide device S1840 at four representative temperatures and a duty cycle of 15.5%. The inset shows a typical emission spectrum of this device.

was focussed onto the input slit of a grating spectrometer (Jobin–Yvon, $d_{\text{focal}}=0.3$ m).

In Fig. 1, we present a series of $L-I-V$ curves of the junction up mounted laser S1840 with InP top cladding. The cavity length was 3 mm and a stripe width of 28 $\mu$m was used. At $-30$ °C and for 15.5% duty cycle, a maximal average power of 115 mW was seen; the threshold current density under these conditions was on the order of 2.68 kA/cm$^2$. At 30 °C, the corresponding numbers are 47 mW and 3.72 kA/cm$^2$; this was already slightly lower than the maximal power of 54 mW at 11.5%. As shown in the inset of Fig. 1, the emission wavelength of this laser was around 1070 cm$^{-1}$, or 9.3 $\mu$m. Because of the vertical transition used, the wavelength did not change at higher current injection. At low duty cycle (1.5%), we observed peak powers of 1.6 W ($dP/dI=387$ mW/A) for $-30$ °C and 1.0 W ($dP/dI=300$ mW/A) at 30 °C. This exceptional performance is due to specific improvements in the design of the active region. The slope efficiency benefits from both the high injection efficiency and the short lower state lifetime of the lasing transition. From the threshold currents at the two extreme temperatures, we deduced a $T_0$ value of 214 K.

Figure 2 shows thermal roll-over average power vs duty cycle curves for normal pulsed operation at two typical temperatures. The duty cycle with the highest average power was 15.5% for $-30$ °C and 11.5% for 30 °C. The maximal power values are 115 mW for $-30$ °C and 54 mW for 30 °C.

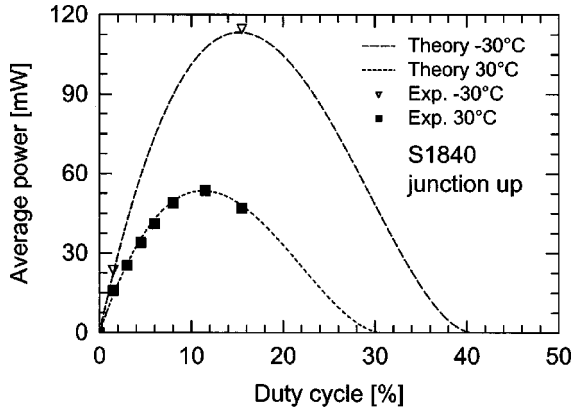


FIG. 2. Thermal roll-over average power vs duty cycle curves of the device S1840 at $-30$ °C and 30 °C. The dashed lines correspond to the theoretical fit using a thermal resistance value of 8.62 K/W.

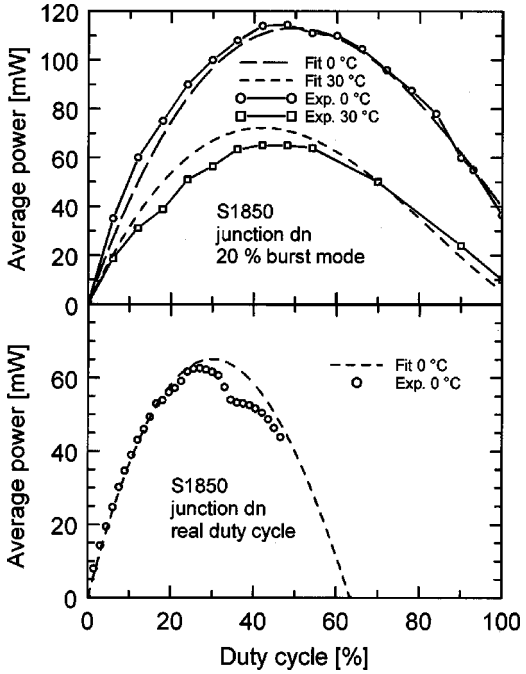


FIG. 3. Thermal roll-over average power vs duty cycle curves of the device S1850 at 0 °C and at 30 °C for burst mode (top) and for normal pulsed operation (bottom). A burst duty cycle of 20% and a repetition frequency of 10 kHz were used for this experiment. The dashed lines are theoretical fits using a thermal resistance value of 2.9 K/W (burst) and 5.67 K/W (normal).

A simple mathematical model allowed the numerical determination of the thermal resistance of this laser.[8] It starts with known quantities such as input electrical power, threshold current, operating voltage, duty cycle, and uses the thermal resistance of the device as a fit parameter. With the curves shown in Fig. 2, we found a value of $R_{\text{th}}=8.62$ K/W for the total (i.e., laser and holder) thermal resistance. The corresponding theoretical curves for the maximal power are also displayed in Fig. 2 (dashed lines); they agree well with the experimental findings. The above $R_{\text{th}}$ value can be reduced considerably when mounting the device junction down directly on a copper heatsink. In the case presented, the heat needs to be transferred through the 150 $\mu$m thick InP substrate and a 2 $\mu$m thick In solder layer to reach the heatsink. When using the junction down mounting technique, the active region is only 2.5 $\mu$m away from the wafer surface, which is soldered onto the heatsink. An even further improvement of the thermal behavior at high duty cycle operation is expected when using BH lasers. In this case, the active region is entirely embedded in InP, which will lead to a very efficient heatsinking.

Similar experiments as shown for S1840 were made with the slightly lower doped, junction down mounted sample S1850. Due to the lower doping in the active region, it showed lower output powers and slope efficiencies; however, the threshold current density was somewhat better than the one of S1840. At low duty cycle, a 3 mm long and 28 $\mu$m wide laser exhibited 147 mW/A at $-30$ °C ($j_{\text{th}}=2.44$ kA/cm$^2$) and 120 mW/A at 30 °C ($j_{\text{th}}=3.0$ kA/cm$^2$). Because of the copper heatsink being somewhat longer than the laser cavity, the lower slope efficiency might be partly due to a shadowing effect. A $T_0$ value of 226 K was calculated for this device.

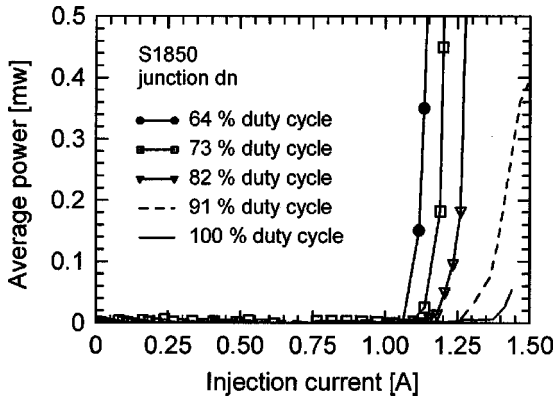


FIG. 4. Light vs current and voltage vs current curves for a 1.5 mm long and 28 $\mu$m wide device S1850 with double-sided facet coating at five different duty cycles between 64% and 100% and at $-27$ °C.

If such a device is operated at high duty cycle, the Peltier cooler, which can dissipate 20 W of thermal power, can reach the limit of its capabilities. This is the reason why we tested our lasers also in burst mode. In Fig. 3, we compare the device performance of S1850 at high duty cycle in normal pulsed operation and in burst mode operation. In 20% burst mode, the thermal load on the Peltier cooler is reduced considerably, because the laser is in ''normal'' pulsed mode only during 20 $\mu$s; this short period is followed by a 80 $\mu$s long time during which the device remains unbiased. As shown in the upper part of Fig. 3, the duty cycle within the burst could be cranked up to a value of 100% (which corresponds to 20% ''real'' pulsed operation) for both 0 °C and 30 °C. The maximal average power during the burst was 112 mW for 0 °C and 60 mW for 30 °C. At 100% duty cycle within the burst, average powers of 36 and 10 mW were obtained for 0 °C and 30 °C, respectively. As with device S1840, we calculated the thermal conductance of the laser and found a value of 410 W/cm$^2$ K ($R_{\mathrm{th}}=2.9$ K/W). The lower half of Fig. 3 shows the measurements at real pulsed operation. Here, the maximal thermal roll-over output power for 0 °C (66.5 mW) was reached already at 27% duty cycle. The dashed line corresponds to the simulated curve using a total thermal resistance value of $R_{\mathrm{th}}=5.67$ K/W. The thermal resistance difference between regular pulsed operation and burst mode corresponds to the thermal resistance of the laser submount. It is obvious that the latter contributes still a considerable fraction, namely almost 50%, to the total thermal resistance. In addition, the deviation of the experimental points from the theoretical curve around 40% duty cycle is probably an indication of an early device aging process.

In Fig. 4, we show $L-I-V$ curves of a different S1850 device. This particular laser had a length of only 1.5 mm. High reflection facet coatings (55% reflectivity) were used to maintain a low threshold current density. In order to protect the device from catastrophic failure, the measurement was always stopped after having reached threshold. At a temperature of $-27$ °C (245 K), this laser could be operated under continuous wave (CW) conditions with a threshold current of 1.38 A ($j_{\mathrm{th}}=3.3$ kA/cm$^2$). The threshold current increased considerably when going from 1.5% ($I_{\mathrm{th}}=0.95$ A) via 65% ($I_{\mathrm{th}}=1.1$ A) up to 100% duty cycle ($I_{\mathrm{th}}=1.38$ A). When taking into account the $T_0$ value just discussed, this threshold current increase allows us to calculate the approximate temperature increase $\Delta T$ in the active region. The relatively high value of $\Delta T=85$ K illustrates that the active region suffers from a thermal stress which might be play an important role for device failure.

In conclusion, we have presented QC lasers at an emission wavelength of 9.3 $\mu$m with InP top cladding layers and both junction up and junction down mounting. Especially the junction down device showed a reasonable thermal resistance value and could be operated CW at $-27$ °C. Maximal average output powers of 115 mW at $-30$ °C and 54 mW at 30 °C were seen for the junction up laser.

The authors gratefully acknowledge Michel Rochat and Stéphane Blaser for technical assistance. This work was financially supported by the Swiss National Science Foundation and the Science Foundation of the European community under BRITE/EURAM projects UNISEL (No. CT97-0557) and SUPERSMILE.

[1] J. Faist, F. Capasso, D. L. Sivco, A. L. Hutchinson, and A. Y. Cho, Science **264**, 553 (1994).
[2] D. Hofstetter, J. Faist, M. Beck, A. Müller, and U. Oesterle, Appl. Phys. Lett. **75**, 665 (1999).
[3] C. Gmachl, J. Faist, J. N. Baillargeon, F. Capasso, C. Sirtori, D. L. Sivco, S.-N. G. Chu, and A. Y. Cho, IEEE Photonics Technol. Lett. **9**, 1090 (1997).
[4] B. Mizaikoff, C. S. Murthy, M. Kraft, V. Pustogow, A. Müller, D. Hofstetter, J. Faist, and N. Croitoru, Proceedings of the PITTCON 2000 Conference, New Orleans, LA, Session 185, 1418.
[5] A. Tredicucci, F. Capasso, C. Gmachl, D. L. Sivco, A. L. Hutchinson, and A. Y. Cho, Appl. Phys. Lett. **73**, 2101 (1998).
[6] A. Tredicucci, F. Capasso, C. Gmachl, D. L. Sivco, A. L. Hutchinson, A. Y. Cho, J. Faist, and G. Scamarcio, Appl. Phys. Lett. **72**, 2388 (1998).
[7] C. Gmachl, A. M. Sergent, A. Tredicucci, F. Capasso, A. L. Hutchinson, D. L. Sivco, J. N. Baillargeon, S. N. G. Chu, and A. Y. Cho, IEEE Photonics Technol. Lett. **11**, 1369 (1999).
[8] M. Beck, J. Faist, U. Oesterle, M. Ilegems, E. Gini, and H. Melchior, IEEE Photonics Technol. Lett. **12**, 1610 (2000).
[9] X. P. Jiang, H. Temkin, M. MacDonald, R. A. Logan, and D. Coblenz, Electron. Lett. **30**, 1680 (1994).
[10] D. Hofstetter, D. Sun, C. Dunnrowicz, M. Kneissl, and D. W. Treat, IEEE Photonics Technol. Lett. **10**, 1371 (1998).
[11] D. Hofstetter, M. Beck, T. Aellen, and J. Faist, Appl. Phys. Lett. **78**, 396 (2001).
[12] J. Faist, C. Sirtori, F. Capasso, D. L. Sivco, J. N. Baillargeon, A. L. Hutchinson, and A. Y. Cho, IEEE Photonics Technol. Lett. **10**, 1100 (1998).